EARTH'S CRYOSPHERE
SCIENTIFIC JOURNAL

Earth`s Cryosphere, 2017, vol. XXI, No. 3, pp. 23–29 **http://earthcryosphere.ru/**

ICE AND FROZEN GROUND PROPERTIES

DOI: 10.21782/EC2541-9994-2017-3(23-29)

THERMAL DEFORMATION OF FROZEN SOILS: ROLE OF WATER AND GAS SATURATION

L.T. Roman[1], V.P. Merzlyakov[2], A.N. Maleeva[1]

[1]*Lomonosov Moscow State University, Department of Geology, 1, Leninskie Gory, Moscow, 119991, Russia; ltr@inbox.ru*
[2]*Sergeev Institute of Environmental Geoscience, RAS, 13, build. 2, Ulansky per., Moscow, 101000, Russia; cryo2@yandex.ru*

Thermal deformation of different components in frozen soil (soil skeleton and pore ice, unfrozen water and gas) is considered theoretically and experimentally. The experiments are applied to frozen sand, silt and clay silt with different moisture contents and gas saturation degrees in the –9 to –1 °C temperature range. Deformation is higher at greater gas saturation. Transient deformation has different relaxation times depending on temperature and grain sizes of soils.

Frozen soils, temperature, strain, moisture, porosity, gas saturation, transient deformation, stationary deformation

INTRODUCTION

Temperature variations cause significant changes to frozen soils, especially those associated with pore water structure and phase transitions. Deformation* is especially sensitive to these changes.

Deformation of soil samples exposed to cooling or heating was investigated previously as a function of grain sizes of soil skeleton, moisture contents, water saturation degrees, and other variables, in more or less successful experiments [*Votyakov, 1963, 1966; Votyakov and Grechishchev, 1969; Grechishchev, 1970; Shusherina et al., 1970, 1973; Shusherina and Krylova, 1977; Grechishchev et al., 1980; Roman, 1987, 2002; Ershov et al., 1989, 2001*]. Porosity was estimated most often at full water saturation. *Ershov et al.* [*1989*] noted that rapidly pre-frozen and slowly cooled soil samples behaved in different ways, while water-undersaturated soil samples experienced smaller thermal expansion or contraction [*Shusherina et al., 1973; Ershov et al., 1989*]. As for gas saturation, it remained overlooked because thermal expansion of gas, though being large in free gas, was assumed to be restrained by stiff skeleton in pore gas.

However, the classical soil mechanics postulates that the same rocks have different properties in the presence and absence of gas-filled porosity, especially as to gas confined in pores and isolated from the atmosphere [*Priklonskiy*, 1949]. The validity of this inference for thermal expansion has been confirmed by studies of frozen peat [*Roman, 1987*]. The relative shares of confined pore gas and gas interacting with the atmosphere control the deformation process, and their role requires further investigation.

In most of the known experiments, samples were cooled in a way to avoid rapid phase change. Generally speaking, samples produce hysteretic deformation patterns at increasing temperatures. Hysteresis is small in sand exposed to sufficiently prolonged effect of low temperatures but becomes significant at higher temperatures.

Dilation-temperature curves have characteristic peaks at which the linear expansion coefficient α changes sign (positive to negative or back) and intervals of monotonous expansion or contraction, each corresponding to certain physical processes and having its features. Other properties, such as strength, can be expected to have different time-dependent patterns as well.

The state of a sample in the beginning of tests depends on its pre-history. Therefore, the behavior of samples within the same intervals will be different at different conditions, e.g., in the case of perturbations to uniform temperature rise, such as stepwise temperature changes or switch between heating and cooling.

* Deformation is considered below in the absence of external forces. Thermal expansion is used in the conventional meaning, positive for expansion and negative for contraction.

During stepwise temperature changes, the temperature field, stress*, and other related properties of frozen soils tend to achieve the stationary state (stabilize), which is recorded in curves of transient strain. The time required for arriving at stationary deformation is the maximum relaxation time of the respective processes [*Grechishchev, 1970; Merzlyakov, 2012*].

THERMAL STRAIN OF DIFFERENT FROZEN SOIL COMPONENTS

According to thermodynamic principles, the strain of individual components of frozen soil in the free state produced by ΔT temperature change is

$$\varepsilon_c = \alpha \Delta T, \quad (1)$$

for solid crystalline particles (including ice), where $\alpha \approx (1–6)\cdot 10^{-5}$ deg^{-1} is the linear expansion coefficient; and

$$\varepsilon_{ph} = \beta \frac{\partial W_w}{\partial T} \Delta T, \quad (2)$$

for pore water subjected to phase change (freezing water and melting ice) [*Merzlyakov, 1980*], where $\beta = -\frac{1}{3}(v_i - v_w)(1-n)\rho_d$; v_i = 1.091 cm^3/g is the specific volume of ice; v_w = 1.0 cm^3/g is the specific volume of unfrozen water; n is the soil porosity; W_w is the moisture content (unfrozen water); ρ_d is the density of dry soil, g/cm^3. At ρ_d = 1.36 g/cm^3 and n = 0.5, the factor β is about –0.02. With the derivative $\frac{\partial W_w}{\partial T} \approx 0.03$ deg^{-1} for silt and clay silt at –1 °C, the strain is $\varepsilon_{ph} \approx -6\cdot 10^{-4} \Delta T$.

Equation (2), with positive and negative strain as conventional, gives the size decrease (contraction) upon warming and increase (expansion) upon cooling.

Estimates show that the free strain of the gas component in frozen soils, within the experimental temperature range, can be calculated as

$$\varepsilon_g = \gamma \Delta T, \quad (3)$$

where $\gamma \approx \frac{1}{3}\frac{1}{273.15\,\text{K}} = 1.22\cdot 10^{-3}$ deg^{-1}.

In equations (1)–(3), T is the Kelvin temperature (K); $\beta \frac{\partial W_w}{\partial T}$ and γ, are linear expansion coefficients like α. Correspondingly, factor 1/3 in (2) and (3) converts volumetric to linear strain.

The strain patterns of individual soil components given by equations (1), (2) and (3) are incompatible. Their compatibility requires the formation of variable internal stress which will affect the strain of bulk samples. The concept of strain compatibility is of special importance and can be illustrated with a simple example. Let three parallel bars of the same length, made of different materials, aligned along their left ends, undergo the same temperature change ΔT. If the bars are disconnected, they have different axial strains because of α difference (incompatible strain). However, if they are connected, the strain will be the same (compatible), but $\varepsilon_s \neq (\alpha_1 + \alpha_2 + \alpha_3) \times \times \Delta T$. This simple example is valid for continuous solids, while the presence of pores and inclusions creates numerous additional forms of incompatibility. Therefore, the strain of a bulk sample exposed to temperature changes is not the sum of strain values for its individual components.

As for the gas component, its strain matters much less than that of the host soil skeleton or ice if the gas is confined. From equation (3) it follows that pore pressure will increase as the temperature of the confined gas increases. This may lead to additional skeleton deformation.

Imagine a thin-walled tube filled with gas. A gas pressure change (Δp) will lead to stress change in the tube wall: $\Delta\sigma = \Delta p d/(2\delta)$, where d is the tube diameter and δ is the wall thickness. Imagine, correspondingly, that the tube diameter is an average size of a close pore while the wall thickness is the respective size of soil skeleton. At Δp = 10 kPa, d = 1 mm, and δ = 10 μm, the stress change reaches $\Delta\sigma$ = 500 kPa, and the strain estimates obtained with and without regard for stress will differ markedly. The example is illustrative, though this is not necessarily always the case. Strain in soil skeleton may also increase indirectly, by other mechanisms.

MATERIALS AND METHODS

Experiments were applied to soils of three types with different particle sizes: sand, silt, and clay silt. Alluvial sand and silt were sampled from an outcrop in the high bank of the Chara River (Northern Transbaikalia). Clay silt was sampled from the Yen-Yakha oil-gas-condensate field. Samples were made as pastes with pre-specified density and water contents, with water undersaturation allowing rather high gas contents. The particle size distribution was estimated by hydrometry and sieving (Table 1) according to State Standard [*2008*]. See Table 2 for water contents of different kinds in the silt and clay silt samples and Table 3 for average values of physical parameters.

The contents of unfrozen water were estimated as in [*Roman, 2002*] and plotted as a function of temperature and initial water content (Fig. 1).

The samples were molded as 90 mm high cylinders, 35 mm in diameter, and compacted layer by

* Temperature-dependent stresses arising in relaxometer [*Grechishchev et al., 1980*] differ from those due to basically different patterns of forces, creep, and consolidation (in the case of compression) [*Vlasov et al., 1998*].

Table 1. **Particle size distribution (%) of clay and sand soils**

Soil types according to State Standard [*2013*]	Size fraction, mm									
	10–5	5–2	2–1	1–0.5	0.5–0.25	0.25–0.1	0.1–0.05	0.05–0.01	0.01–0.005	<0.005
Fine silt*	–	0.93	1.10	2.50	1.28	1.90	3.07	61.30	24.91	3.01
Light-textured clay silt*	–	–	–	–	–	0.22	10.33	22.37	27.74	39.34
Medium sand**	0.40	2.02	4.11	35.40	56.97	0.47	0.63***	–	–	–

* Measured by hydrometry
** Measured by sieving
*** Size fraction <0.1 mm.

Table 2. **Moisture contents of different kinds in silt and clay silt samples**

Soil type	Limit moisture contents		Plastic index I_p
	Plastic limit W_P	Liquid limit W_L	
Fine silt	0.20	0.26	0.06
Light-textured clay silt	0.21	0.32	0.11

Table 3. **Physical parameters of soils, average values**

Soil type	W_{tot}	W_f	Density, g/cm^3			e	S_r	S_w/S_g at θ			
			ρ_s	ρ	ρ_d			–7 °C	–5 °C	–3 °C	–1 °C
Sand	0.10	0.31	2.65	1.59	1.45	0.83	0.32	0.35 / 0.65	0.35 / 0.65	0.34 / 0.66	0.34 / 0.66
	0.15	0.34		1.60	1.39	0.90	0.44	0.48 / 0.52	0.48 / 0.52	0.47 / 0.53	0.47 / 0.53
	0.20	0.34		1.68	1.40	0.89	0.59	0.64 / 0.36	0.64 / 0.36	0.64 / 0.36	0.64 / 0.36
Silt	0.20	0.35	2.70	1.65	1.37	0.97	0.56	0.60 / 0.40	0.60 / 0.40	0.60 / 0.40	0.58 / 0.42
	0.22	0.36		1.66	1.36	0.98	0.60	0.65 / 0.35	0.65 / 0.35	0.64 / 0.36	0.63 / 0.37
	0.25	0.38		1.66	1.32	1.04	0.65	0.70 / 0.30	0.70 / 0.30	0.69 / 0.31	0.68 / 0.32
Clay silt	0.20	0.32	2.71	1.74	1.45	0.87	0.62	0.67 / 0.33	0.66 / 0.34	0.66 / 0.34	0.65 / 0.35
	0.25	0.34		1.76	1.41	0.92	0.73	0.79 / 0.21	0.78 / 0.22	0.78 / 0.22	0.76 / 0.24
	0.30	0.39		1.71	1.32	1.06	0.77	0.82 / 0.18	0.82 / 0.18	0.81 / 0.19	0.79 / 0.21

Note. W_{tot} is total moisture, u.f.; W_f is moisture content at total moisture capacity, u.f.; ρ_s is density of soil particles, g/cm^3; ρ is density of frozen soil, g/cm^3; ρ_d is density of dry soil, g/cm^3; e is porosity; S_r is saturation, u.f.; S_w is pore filling with water and ice, u.f.; S_g is pore filling with gas, u.f.; θ is soil temperature, °C.

layer. The inner surface of the mold was pre-lubricated with petrolatum and the outer surface was thermally insulated to ensure uniform freezing propagation normally to the sample axis. The molds were additionally insulated with water-proof polyethylene film to prevent soil drying. To avoid moisture migration during the experiment, the samples were pre-frozen in a cooling chamber at –25 °C for at least 24 hours. Strain (displacement) sensors were mounted on plastic plates frozen into the cleaned top and base surfaces of the cylinders taken out of the molds (Fig. 2).

Vertical displacement was measured by ASIS sensors. The samples were placed in a box insulated with Caprolon in order to cancel the effect of cooling chamber inertia. The sensors were fixed tightly on the sample surfaces and in the box cover. The temperature was measured in the chamber and in additional samples of each soil type which did not carry displacement sensors.

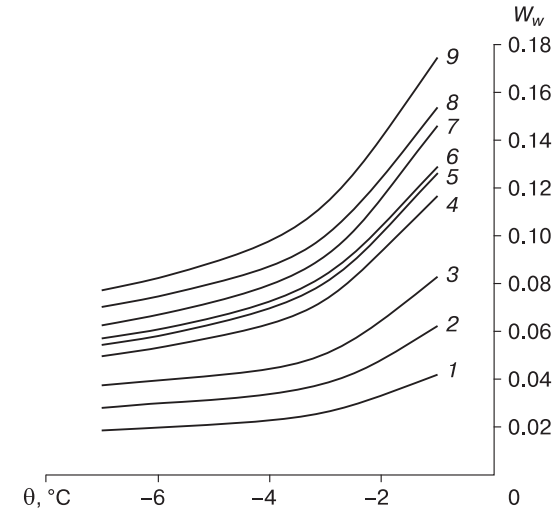

Fig. 1. Contents of unfrozen water (W_w) in analyzed soil samples as a function of temperature and initial water content:

1 – 0.10; *2* – 0.15; *3* – 0.20 (for sand); *4* – 0.20; *5* – 0.22; *6* – 0.25 (for silt); *7* – 0.20; *8* – 0.25; *9* – 0.30 (for clay silt).

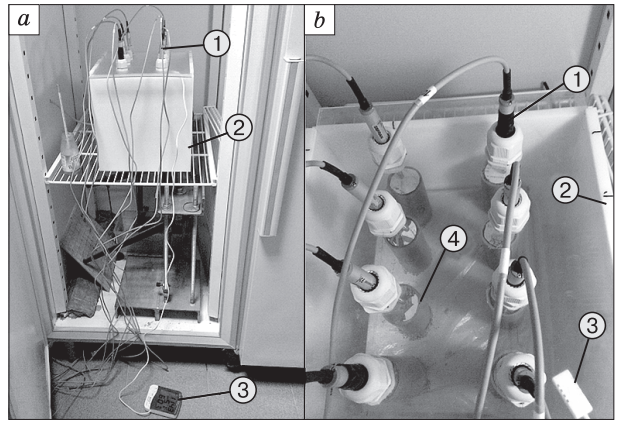

Fig. 2. System for measuring thermally-induced deformation.

a: general view; *b*: top view; 1 = sensors; 2 = thermal insulation; 3 = electronic thermometer; 4 = sample.

Temperature was increased stepwise from –9 to –1 °C, with the steps –7, –5, –3 and –1 °C. Displacement of the sample top was counted from the beginning of each temperature step at every 10 s (6 measurements), 1 min (5 measurements), 5 min (5 measurements), 10 min (3 measurements), 30 min (8 measurements), 1 h (19 measurements), and 4 hours (14 measurements). Then the measurements were taken at 7 h till strain rate stabilization, according to the criterion 0.001–0.002 mm for 12–14 h.

All tests were run in triplicate. The results were statistically processed according to State Standard [*2012*].

RESULTS

The measured displacements were used to plot time-dependent transient strain caused by temperature change, for each temperature step. Relative expansion was assumed positive, contrary to the con-

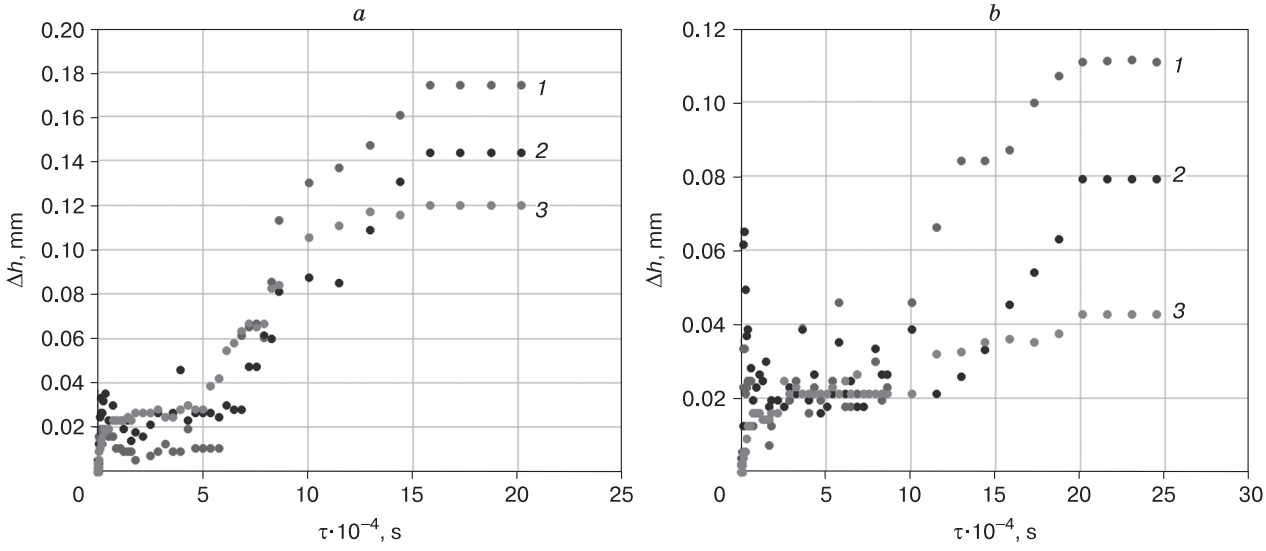

Fig. 3. Time-dependent (τ) height changes (Δ*h*) in a silt sample:

Panels *a* and *b* are for temperatures from –9 to –7 °C and –3 to –1 °C, respectively; curves *1* to *3* are total moisture contents: *1* – W_{tot} = 0.20; *2* – W_{tot} = 0.22; *3* – W_{tot} = 0.25.

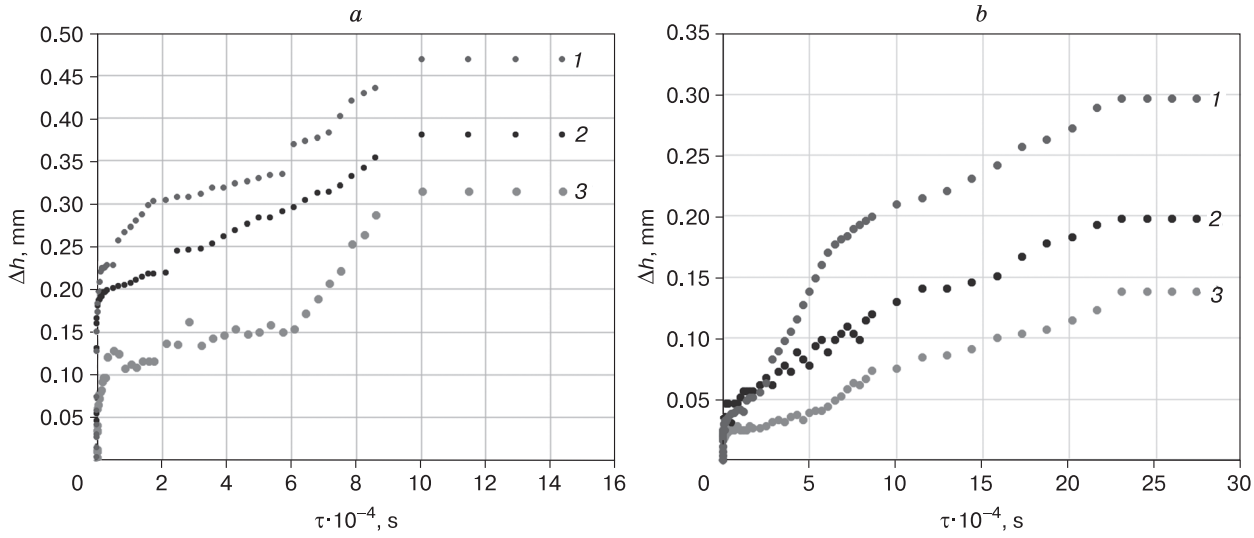

Fig. 4. Time-dependent (τ) height changes (Δ*h*) in a silt sample:

Panels *a* and *b* are for temperatures from –9 to –7 °C and –3 to –1 °C, respectively; curves *1* to *3* are total moisture contents: *1* – W_{tot} = 0.10; *2* – W_{tot} = 0.15; *3* – W_{tot} = 0.20.

ventional assumption in continuous mechanics and in the theory of material strength.

At early times (Fig. 3), the silt samples show considerable scatter irrespective of total moisture content, especially at lower temperatures (Fig. 3, *a*), possibly, because of randomness in non-equilibrium phase transitions. In our experiments, the variations were still more chaotic in clay silt but no such effect was observed in sand (Fig. 4). The characteristic relaxation times for each soil type do not depend on total moisture content W_{tot} within its considered range.

The curves were then changed to plots of stationary strain increment at the respective temperature steps:

$$\Delta\varepsilon_i = \Delta h_i / h_{i-1}, \qquad (4)$$

where $\Delta h_i = h_i - h_{i-1}$ is the stable sample height increment (displacement) at the end of the temperature step (θ_i, °C); h_{i-1} is the sample height in the beginning of the temperature step (θ_{i-1}, °C), i = 1, 2, 3, 4.

The stationary strain increment is plotted against gas saturation in Fig. 5 at successive temperature steps (°C). The strain increment at each step varies with water saturation and pore gas volume: it is higher at lower moisture contents and higher gas contents, especially at low temperatures.

Linear thermal expansion coefficients were calculated as relative changes in the characteristic size of samples free from external loads, at 1 °C temperature increase:

$$\alpha_i = \frac{\Delta h_i}{h_{i-1}}\left(\theta_i - \theta_{i-1}\right). \qquad (5)$$

Thus estimated coefficients at each temperature step for soils of different types and total water contents are listed in Table 4.

Thus the experiments demonstrate that the strain behavior in soil samples pre-frozen at –25 °C and exposed to warming to above –10 °C, in the absence of external loads, depends on gas saturation.

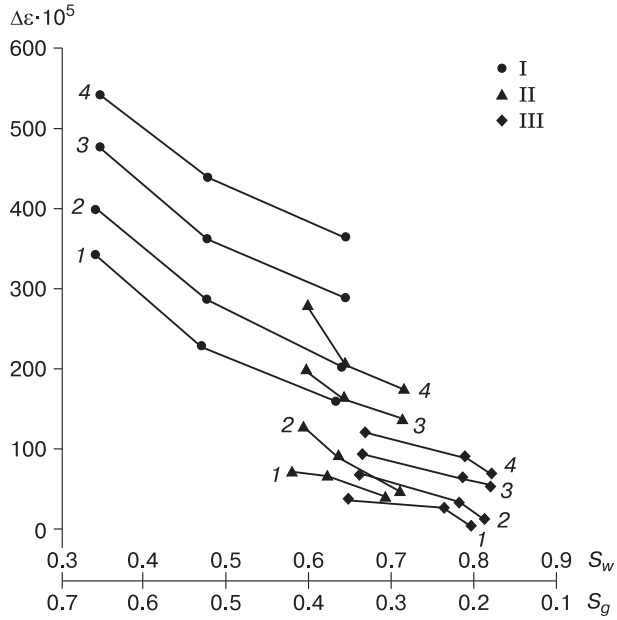

Fig. 5. Water and gas saturation (S_w, S_g) dependences of stationary strain increment in the temperature range from –9 to –1 °C:

I – sand; II – silt; III – clay silt. Temperature steps: –1 °C (*1*); –3 °C (*2*); –5 °C (*3*); –7 °C (*4*).

Table 4. **Thermal expansion coefficients in different temperature ranges for different soil types and moisture contents**

W_{tot}	$\alpha \cdot 10^5$, deg^{-1}			
	–9 to –7 °C	–7 to –5 °C	–5 to –3 °C	–3 to –1 °C
		Sand		
0.10	271	240	200	172
0.15	220	182	143	115
0.20	182	145	101	80
		Silt		
0.20	140	101	65	36
0.22	104	83	46	34
0.25	88	70	25	22
		Clay silt		
0.20	61	47	35	20
0.25	45	32	19	14
0.30	35	28	7	2.5

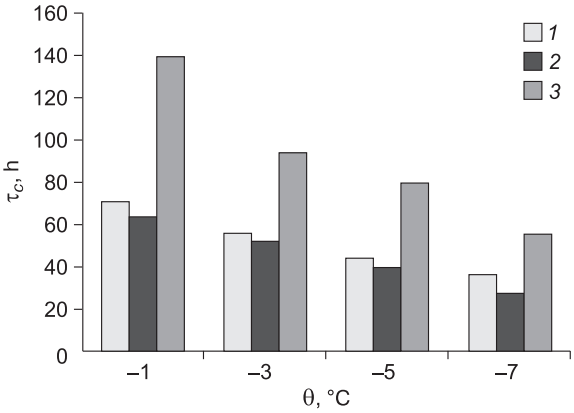

Fig. 6. Histogram showing relaxation time (τ_c) of deformation in silt (*1*), sand (*2*), and clay silt (*3*).

Data series correspond to temperature steps of θ changes.

This effect is primarily due to the confined gas phase (air or water vapor). Phase change of pore water causes minor influence in sand, but this influence is apparently greater in silt and clay silt, which may explain small strain in the latter.

Figure 6 shows relaxation times for sand, silt, and clay silt at four successive temperature steps. The relaxation times are the shortest in sand but longer in finer-grained samples which experience decay of stress related to transient strain. Stepwise soil warming to –7, –5, –3, and –1 °C likewise increases the relaxation time with increasing contents of unfrozen pore water: it becomes approximately twice longer for soils of the same type upon temperature rise from –9 to –1 °C.

CONCLUSIONS

The reported experimental results and numerical estimates lead to the following inferences.

1. Strain of individual components in frozen soil exposed to temperature change is not additive, i.e., strain of a sample is not the sum of strain values for its individual components.

2. Stationary strain at the respective warming steps, in the temperature range from –9 to –1 °C, is higher at higher gas saturation and lower water saturation.

3. Strain in frozen soil is higher at greater gas saturation at the same temperature, possibly because of air and water vapor confinement in the pores.

4. Relaxation times of transient strain are longer in soil types of smaller particle sizes at the same temperature and in warmer samples of the same soil types. In this case, the relaxation time becomes about twice longer as the temperature rises from –9 to –1 °C.

We wish to thank M.N. Tsarapov and P.I. Kotov from the Subdepartment of Geocryology at Moscow State University for aid in experimental work.

The study was supported by grant 15-05-0491/15 from the Russian Foundation for Basic Research.

References

Ershov, E.D., Cheverev, V.G., Nikolaeva, G.V., Brouchkov, A.V, Shevchenko, L.V., 1989. The nature of anomalous thermally-induced deformation in frozen soils, in: Geocryological Studies, Moscow University Press, Moscow, pp. 171–182. (in Russian)

Ershov, E.D., Komarov, I.A., Brushkov, A.V., Hors, M.A., 2001. Thermally-induced deformation of ice-rich fine-grained permafrost at low negative temperatures, in: Proc. 2nd Conf. of Russian Permafrost Scientists. Moscow University Press, Moscow, pp. 81–87.

Grechishchev, S.E., 1970. Fundamentals of Predicting Thermally-Induced Stress and Strain in Permafrost. VSEGINGEO, Moscow, 53 pp. (in Russian)

Grechishchev, S.E., Chistotinov, L.V., Shur, Yu.L., 1980. Cryogenic Physico-Geological Processes and their Prediction. Nedra, Moscow, 382 pp. (in Russian)

Merzlyakov, V.P., 1980. Effect of unfrozen water on thermally-induced deformation of clayey soils. Izv. Vuzov. Stroistelstvo i Arkhitektura, No. 8, 20–24.

Merzlyakov, V.P., 2012. Thermal expansion as a parameter of frozen ground. Geoekologiya, No. 2, 159–167.

Priklonskiy, V.A., 1949. Soil Science. Part 1. Gos. Izd. Geol. Lit., Moscow, 410 pp. (in Russian)

Roman, L.T., 1987. Frozen Peat-Bearing Soils as a Foundation for Construction. Nauka, Novosibirsk, 219 pp. (in Russian)

Roman, L.T., 2002. Mechanics of Frozen Ground. MAIK Nauka/Interperiodika, Moscow, 426 pp. (in Russian)

Shusherina, E.P., Barkovskaya, E.N., Revina, L.A., 1973. Deformation of frozen fine-grained rocks controlled by their compositions and temperature variations from –0.5 to –55 °C, in: Permafrost Studies, Moscow University Press, Moscow, Issue XIII, pp. 212–227. (in Russian)

Shusherina, E.P., Krylova, L.S., 1977. Thermally-induced deformation of frozen ground, in: Permafrost and Snow. Nauka, Moscow, pp. 70–81. (in Russian)

Shusherina, E.P., Rachevskiy, B.S., Otroshchenko, O.P., 1970. Studies of thermally-induced deformation in frozen ground, in: Permafrost Studies, Moscow University Press, Moscow, Issue X, pp. 273–283. (in Russian)

State Standard, 2008. Working Document GOST 12536-79. Soils. Methods of Laboratory Grain Size Measurements and Soil Structure Determination. IPK Izd. Standartov, 17 pp. (in Russian)

State Standard, 2012. Working Document GOST 20522-2011. Soils. A Method for Statistical Processing of Testing Data. NIIOSP, Moscow, 23 pp. (in Russian)

State Standard, 2013. Working Document GOST 25100-2011. Soils. Classification. Standartinform, Moscow, 38 pp. (in Russian)

Vlasov, A.N., Lisin, L.D., Merzlyakov, V.P., Talonov, A.V., 1998. On the possibility of filtration consolidation of plastic frozen silt. Kriosfera Zemli II (2), 65–68.

Votyakov, I.N., 1963. Thermal expansion of frozen soils, in: Strength and Creep of Frozen Soil. Izd. AN SSSR, Moscow, pp. 157–162. (in Russian)

Votyakov, I.N., 1966. Volumetric changes of fine-grained frozen soil associated with phase change of water at temperature variations, in: Proc. 8th All-USSR Interdepartmental Workshop on Geocryology. Yakutknigoizdat, Yakutsk, pp. 11–21. (in Russian)

Votyakov, I.N., Grechishchev, S.E., 1969. On a temporary aftereffect of thermally induced stress and strain in frozen soil, in: Construction in East Siberia and Extreme North. Krasnoyar. PromstroiNIIproekt, Krasnoyarsk, pp. 41–60. (in Russian)

Received November 10, 2015